

Reduction of Torque Ripple in DTC Induction Motor Drive with Discrete Voltage Vectors

Marko Rosić¹, Borislav Jeftenić², Milan Bebić²

Abstract: This paper presents a practical implementation of direct torque control (DTC) of an induction machine on MSK2812 DSP platform, and the analysis of possibilities for reduction of torque ripple. Basic theoretical background relating the DTC was primarily set and the obtained experimental results have been given. It is shown that the torque ripple can be reduced by adjusting the intensity of voltage vectors and by modification of hysteresis comparator, while the simplicity of the basic DTC algorithm has been maintained.

Keywords: Induction motor drive, Direct torque control, Torque ripple, Hysteresis comparator modification, DSP.

1 Introduction

Direct Torque Control (DTC) is the youngest control technique of AC machines, and has been present for more than two decades [1]. Due to its preferable characteristics, such as quick torque response and simplicity of practical implementation, DTC is considered to be an alternative to the Field Oriented Control (FOC) techniques [2]. DTC algorithm with discrete voltage vectors (classical DTC) presents the simplest form of flux and torque control without rotating coordinate transformation and complicated mathematical calculations. However, the main drawbacks of this algorithm are high torque and current ripple and variable switching frequency [3]. These imperfections have been overcome with more or less complicated algorithms using pulse width modulation (PWM) or space vector modulation (SVM) and PI regulators [4-5]. Thus, the torque ripple has been significantly reduced, to the detriment of bandwidth degradation due to PI regulators and usage of more complex calculation.

This paper shows the analysis of torque and current ripple reduction using DTC with discrete voltage vectors involving modification of hysteresis comparators to obtain adjustable voltage vector intensity. The primary idea is to retain the simplicity of the classical DTC algorithm without PI regulators and coordinate transformations, and to reduce torque ripple and provide constant switching frequency.

¹Faculty of Technical Sciences Čačak, Svetog Save 65, 32000 Čačak, Serbia, E-mail: marko.rosic@ftn.kg.ac.rs

²School of Electrical Engineering, Bulevar kralja Aleksandra 73, 11120 Belgrade, Serbia
E-mails: jeftenic@etf.rs; bebic@etf.rs

2 Theoretical Review of DTC with Discrete Voltage Vectors

The direct torque control of the induction machine with voltage source inverter (VSI) can be achieved by controlling of machine stator flux with optimal switching state selection. Electromagnetic torque of the induction machine depends on the mutual position of stator and rotor flux and can be presented by the following equation:

$$m_e = \frac{3}{2} P \frac{L_m}{L_s L_r - L_m^2} |\Psi_s| \cdot |\Psi_r| \sin(\theta_{\Psi_s} - \theta_{\Psi_r}), \quad (1)$$

where P is the number of pole pairs, L_s , L_r are the stator and rotor inductances, L_m is the mutual inductance; $|\Psi_s|$, $|\Psi_r|$ are the stator and rotor flux magnitudes, and θ_{Ψ_s} , θ_{Ψ_r} are the stator and rotor flux angles with respect to reference axis.

Rotor time constant T_r grows with machine power ($T_r = 0.12$ s, for 2.2 kW induction motor). That explains slow change of rotor flux which can be neglected during the time Δt . In that way, quick change of stator flux in respect to rotor flux enables direct torque control. Stator voltage equation in stationary reference frame is given by (2):

$$\mathbf{u}_s = R_s \mathbf{i}_s + \frac{d\mathbf{\Psi}_s}{dt}, \quad (2)$$

$$\Delta\mathbf{\Psi}_s = \mathbf{u}_s \Delta t, \quad (3)$$

where \mathbf{u}_s , \mathbf{i}_s and $\mathbf{\Psi}_s$ are stator voltage, current and flux vectors respectively, and R_s is stator resistance.

Neglecting the stator resistance R_s , variation of the stator flux $\Delta\mathbf{\Psi}_s$ in (2) can be presented by (3). By selecting one of the eight voltage vectors of the three phase inverter (Fig. 1), it is possible to influence the position of stator flux in respect to the slowly changing rotor flux. The variation of rotor flux magnitude and phase angle can be neglected during the time Δt . This simplification is reasonable since the sampling time ($T_s = \Delta t$), on real-time DSP based systems, is much less than rotor time constant T_r . In this way, the increase or decrease of stator flux intensity or angle, and thus the torque, can be provided by selecting an optimum voltage vector. Increment of the stator flux during the time Δt is illustrated in Fig. 1.

Selection of required voltage vectors depends on the demands for flux and torque (where 1 is increasing demand, -1 is decreasing demand and 0 means no change required) and can be represented by **Table 1**. In **Table 1** k stands for sector number S_k in stationary reference plane where estimated stator flux $\mathbf{\Psi}_s$ is located (Fig. 1).

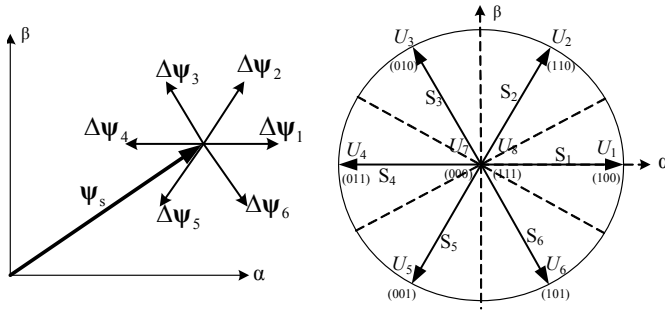


Fig. 1 – Voltage vector impact to the stator flux amplitude and angle variation.

Table 1
Voltage vector selection.

S_ψ	S_m		
	1	0	-1
1	U_{k+1}	U_7 or U_8	U_{k-1}
-1	U_{k+2}	U_7 or U_8	U_{k-2}

Demands for flux S_ψ and torque S_m are obtained from hysteresis comparators which are presented in Fig. 2. Depending on the value of estimated stator flux and torque, demands for increasing $S = 1$, decreasing $S = -1$ or null demand $S = 0$ are generated. Demand $S = 0$ occurs when error Δm lies within torque hysteresis limits.

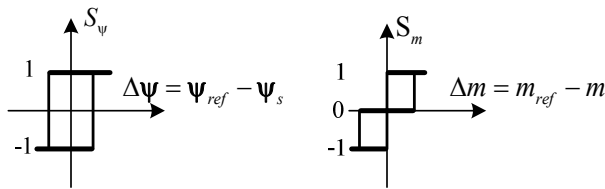


Fig. 2 – Flux hysteresis comparator (left) and torque hysteresis comparator (right).

The accuracy of estimated stator flux directly affects the accuracy of the electromagnetic torque estimation by (4):

$$m_e = \frac{3}{2} P (\psi_{\alpha s} i_{\beta s} - \psi_{\beta s} i_{\alpha s}), \quad (4)$$

where $\psi_{\alpha s}$, $\psi_{\beta s}$ are stator fluxes in stationary $\alpha\beta$ reference frame, and $i_{\alpha s}$, $i_{\beta s}$ are stator currents in stationary $\alpha\beta$ reference frame.

For this reason, accurate estimation of stator flux position is the matter of great importance. Various stator flux estimation methods are subjects of many scientific papers. Great research effort has been made in the realization of flux estimator which will be reliable over a wide speed range. For instance, flux estimators which relies on the machine voltage model has poor characteristics at low speed, due to integration signal contaminated with DC offset. Estimator based on current machine model has satisfactorily results at low speed but poor results at high speed. Method based on a combination of voltage and current model is proved to be reliable method of flux estimation [6]. This estimator provides good accuracy and robustness of estimated flux even with non-ideal machine parameters. Further, it permits flux estimation at all (including zero) speeds and exhibit speed-invariant dynamics which is important for wide speed range drives [7].

Here, the flux estimation is realized with current model estimator by following estimations (5):

$$\begin{aligned} \Psi_{\alpha s} &= \frac{L_s L_r - L_m^2}{L_r} i_{\alpha s} + \frac{L_m}{L_r} \Psi_{\alpha r}, & \frac{d\Psi_{\alpha r}}{dt} &= \frac{R_r L_m}{L_r} i_{\alpha s} - \frac{R_r}{L_r} \Psi_{\alpha r} - \omega_r \Psi_{\beta r}, \\ \Psi_{\beta s} &= \frac{L_s L_r - L_m^2}{L_r} i_{\beta s} + \frac{L_m}{L_r} \Psi_{\beta r}, & \frac{d\Psi_{\beta r}}{dt} &= \frac{R_r L_m}{L_r} i_{\beta s} - \frac{R_r}{L_r} \Psi_{\beta r} + \omega_r \Psi_{\alpha r}, \end{aligned} \quad (5)$$

where R_r is rotor resistance and ω_r is rotor speed.

The reason for this is simplicity of digital implementation and the fact that the application will be tested at low speeds at which current model estimator has good results.

3 Algorithm Implementation on DSP Platform MSK2812

Direct torque control algorithm with discrete voltage vectors was implemented on Technosoft platform MSK2812 [8]. Setup MSK2812 consists of the power module ACPM750 (750W/230V) with rectifier, three phase IGBT inverter bridge and 32-bit digital signal processor TMS320F2812 with fixed point arithmetic. DSP F2812 runs at 150MHz (6.67ns). All quantities used in calculation are represented in Q16 format where 16 bits represent fractional part of a number, 15 bits integer part and 1 bit goes to the number sign.

Induction motor is equipped with two phase incremental encoder with 500 pulses per revolution. Motor parameters for star connection are given in the **Table 2**.

Control algorithm is separated in two loops. Fast loop runs with interrupt at every 50 μ s and performs following calculations: A/D conversion of stator currents, stator flux estimation (5), execution of comparators and voltage vector selection (**Table 1**) which will be used in next sample instant. Slow loop runs

on every 10th interrupt which is 0.5 ms. This loop is responsible for speed measurement, setting of the references for flux and torque, and data collection.

Table 2
SIEBER LS71 motor parameters.

U_n [V]	400	R_s [Ω]	24,6
I_n [A]	0,95	R_r [Ω]	16,1
P_n [W]	370	L_m [H]	1,46
n_n [min^{-1}]	2860	L_s [H]	1,48
p [pole num.]	2	L_r [H]	1,48

Hysteresis comparators width are set to 10% for torque (Mbw), and 1% for flux (Fbw), regarding their motor nominal values. Fig. 3 shows estimated the stator flux and torque obtain for nominal flux reference 0.95 Wb and the torque reference of ± 0.4 Nm.

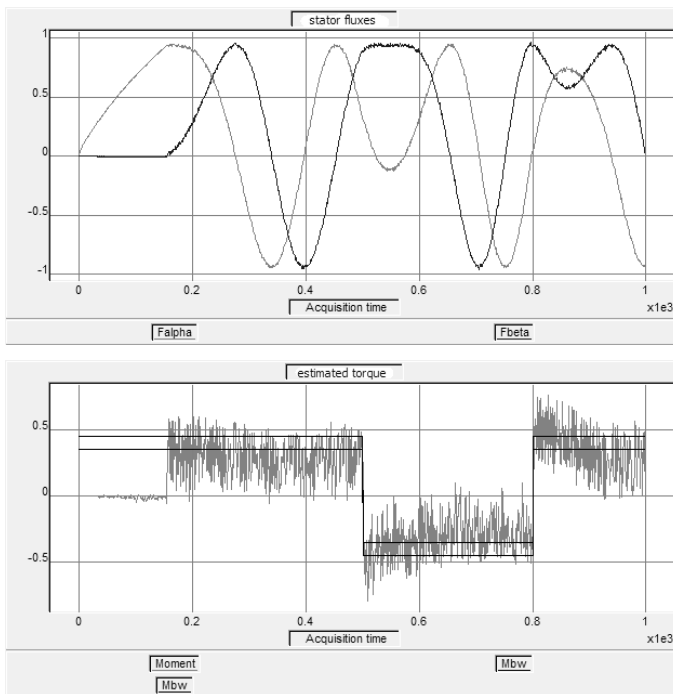


Fig. 3 – Estimated stator flux and electromagnetic torque.

DTC with discrete voltage vectors has a large torque ripple regarding to its nominal value as can be seen in Fig. 3. Limits used in torque hysteresis comparator are marked with two straight lines in Fig. 3. The estimated torque

has a large ripple around these hysteresis limits. Machine pre-magnetizing to the nominal flux is provided by voltage vector in α axes (a phase) in order to avoid high starting currents. After the machine pre-magnetizing, torque demand command is released. Fig. 4 shows circular trajectory of stator flux vector in $\alpha\beta$ reference frame.

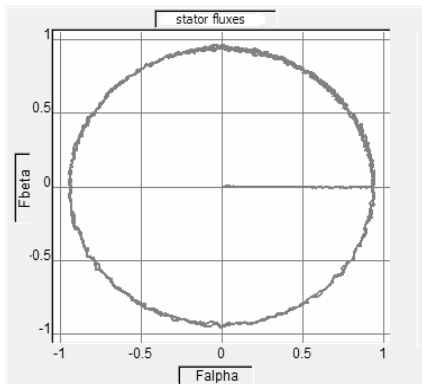


Fig. 4 – Circular trajectory of stator flux vector.

4 Analysis of Possibilities of Torque Ripple Reduction

Papers [9] and [10] show that torque ripple reduction with constant switching frequency is possible by adaptive hysteresis band modification depending on the applied voltage vector. Literature [11] proposes the torque ripple reduction by using the combination of three out of seven voltage vectors during each sampling period.

Unlike the aforementioned methods, hysteresis band modification and adjustment of voltage vector intensity was analyzed in this paper. At the end, modified hysteresis comparator with 6 non-zero voltage vectors with changing intensity was proposed in order to reduce the torque ripple.

4.1 Hysteresis band changing

Fig. 5 shows the estimated torque in case of changing the torque hysteresis band with the torque reference set at 0.4 Nm.

Fig. 5 shows the estimated torque responses with hysteresis band width set to 0.1 Nm, 0.2 Nm and 0.3 Nm respectively (from top to bottom). First diagram shows that torque has ripple of nearly 0.6 Nm and cannot be kept within hysteresis limits. In contrast, reduced torque ripple can be noticed in the last figure with hysteresis band set at 0.3 Nm. This is caused by selection of zero voltage vector during the periods when estimated torque is found within wider hysteresis limits. For this value of hysteresis band width, the estimated torque is

around lower hysteresis limit. When the estimated torque is below the lower hysteresis limit, the voltage vector for increase of torque is applied. Similarly, when the estimated torque is within hysteresis limits, zero voltage vector is applied. Although the torque ripple is reduced, the obtained average torque value is less than the torque reference and does not reach it, which could degrade the drive performance.

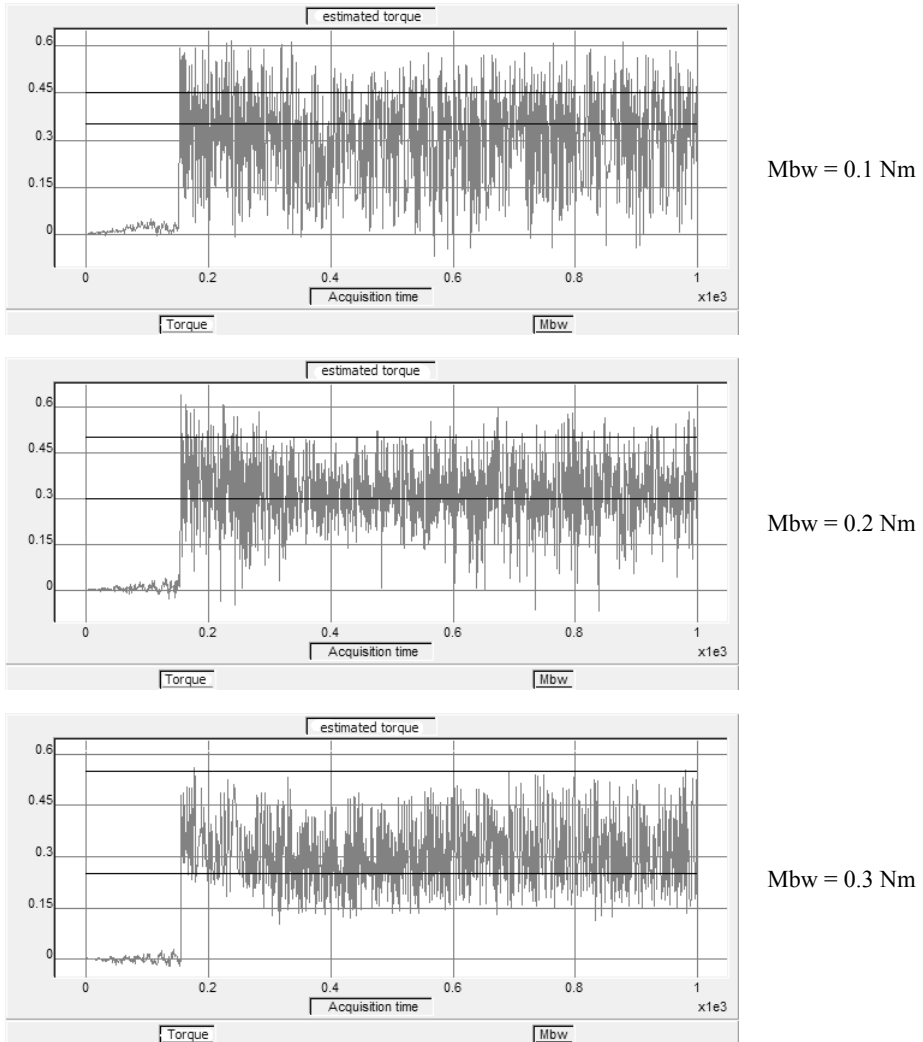


Fig. 5 – Estimated electromagnetic torque with hysteresis band changing.

4.2 Voltage vector intensity adjustment

The presence of large torque and current ripple is the result of full value of the voltage vector (when demand for increase or decrease of torque is active) and hysteresis band (when zero vector is applied). However, if variation in intensity of the six non zero voltage vectors is possible, the stator flux increase in the next sampling period will also be variable, as shown in Fig. 6.

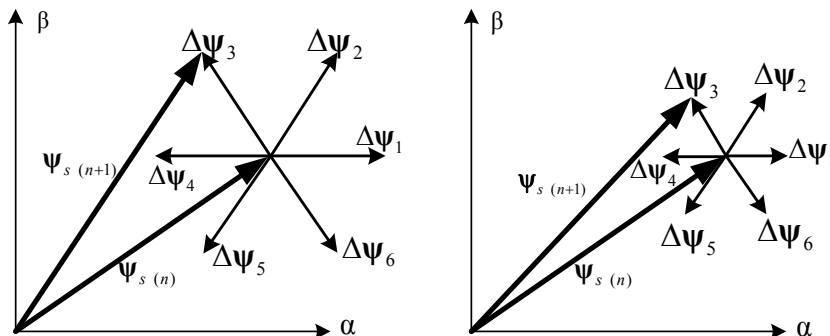
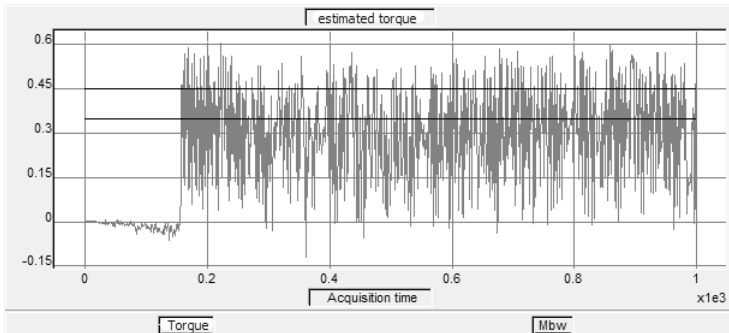


Fig. 6 – Stator flux increase for different voltage vector intensities.

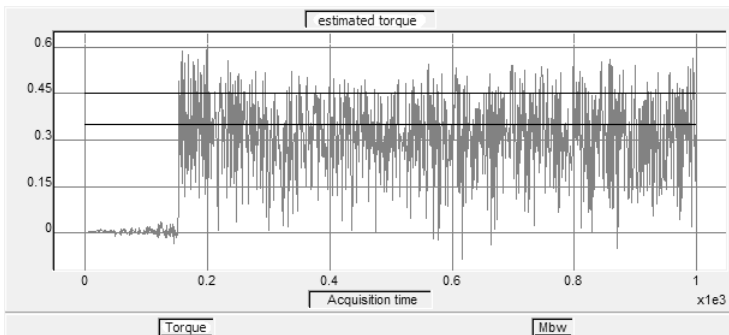
The proposed intensity variation of the six non-zero voltage vectors is based on application of PWM modulation. Each of the six voltage vectors can be adjusted from zero to full value. In this way, instead of having a switching element turned on or off during entire sampling period, it is possible to define the time of its on/off state during this period. This allows defining six non-zero voltage vectors with different intensities, which will be applied to the motor (Fig. 1). The switching frequency becomes constant, involving PWM module of the DSP. In this way it is possible to analyze the DTC drive performance with variable discrete voltage vectors without changing the basic control algorithm principle. Fig. 7 shows the influence of six different voltage vector intensities to the torque ripple.

Fig. 7 shows estimated torque response for the voltage vector intensity set at fixed values of 100%, 90%, 80%, 70%, 60% and 50% of the full voltage vector respectively. It can be clearly seen that the smallest torque ripple corresponds to the 50% of the full voltage vector. This confirms the initial assumption illustrated in Fig. 6 and shows that it is possible to reduce the torque ripple in this way. However, the drawback is slower response to the torque reference because lower intensity voltage vector is available. This drawback can be overcome by using voltage vectors with variable intensities and hysteresis comparator modification which is presented in the following.

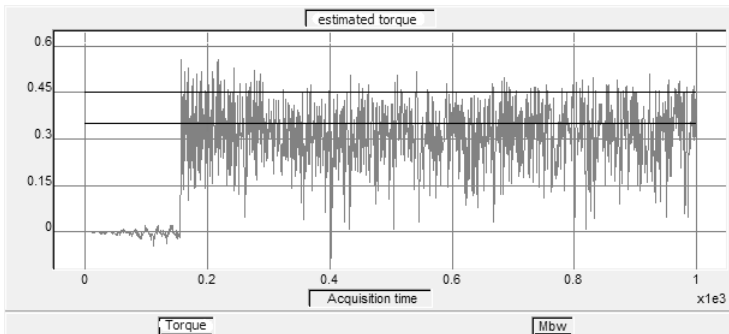
Reduction of Torque Ripple in DTC Induction Motor Drive with Discrete Voltage...



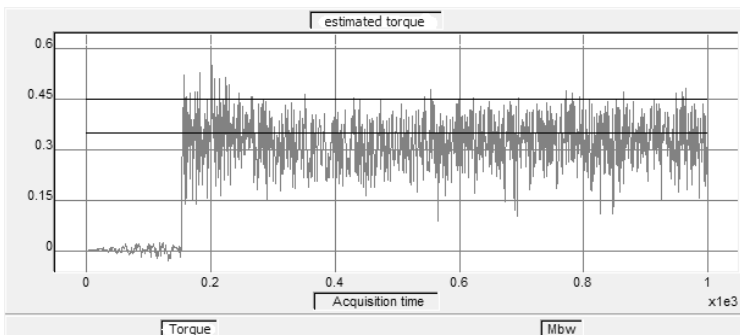
voltage
vector
100%



voltage
vector
90%



voltage
vector
80%



voltage
vector
70%

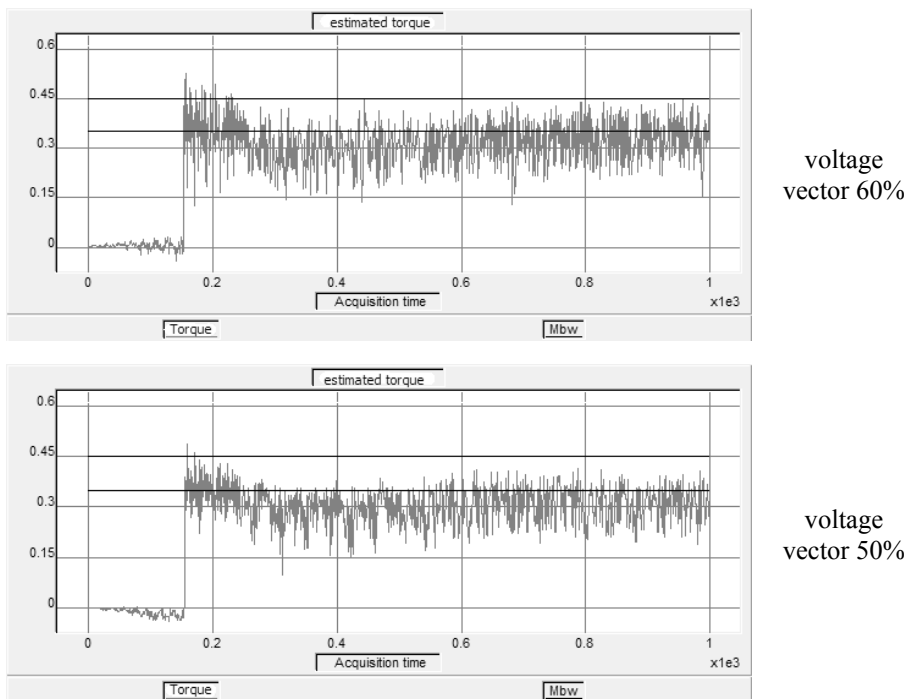


Fig. 7 – Estimated torque response for different voltage vector intensities.

4.3 Hysteresis comparator modification

To provide the use of voltage vectors with variable intensities, a modified hysteresis comparator is proposed. Instead of three level torque comparator (Fig. 2) it is necessary to form multilevel comparator. Fig. 8 shows modified multilevel comparator, with signals from the three-level comparator shown on the left hand side of the arrows.

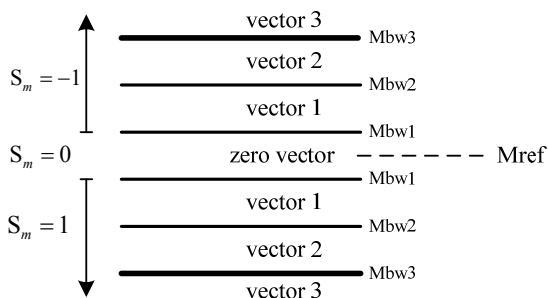
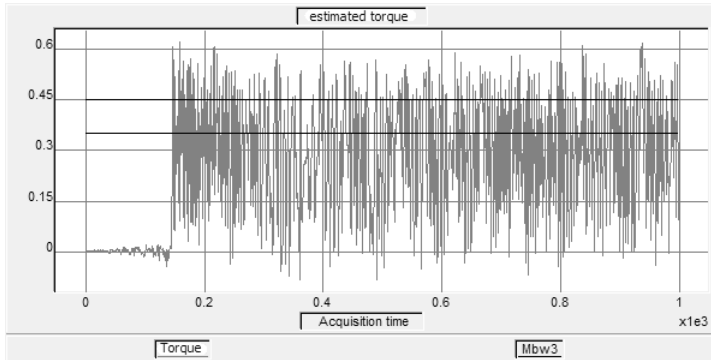


Fig. 8 – Modified torque hysteresis comparator.

In this case comparator is divided into 5 segments with equal width. If estimated torque takes value out of hysteresis band, the largest voltage vector will be applied (vector 3). In this way, depending on torque error, voltage vector of appropriate intensity will be selected. Voltage vector direction remains defined with **Table 1**, depending on flux and torque demands, keeping control algorithm simple.

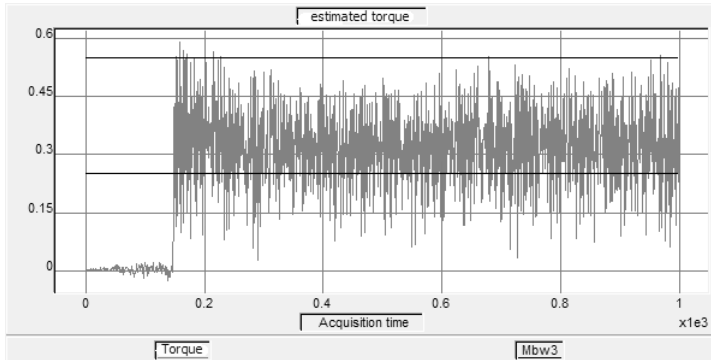


$MbW3 = 0.1 \text{ Nm}$

vector1 = 40%

vector2 = 80%

vector3 = 100%

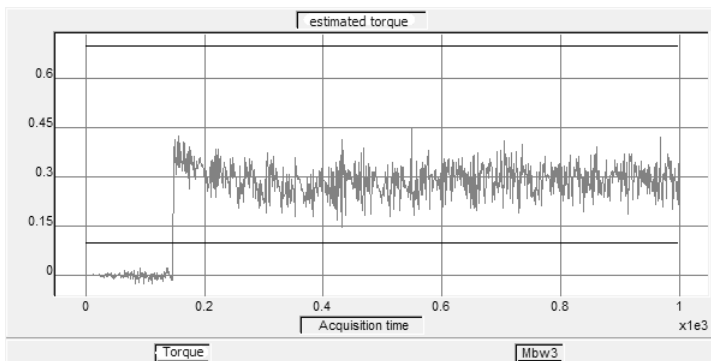


$MbW3 = 0.3 \text{ Nm}$

vector1 = 40%

vector2 = 80%

vector3 = 100%



$MbW3 = 0.6 \text{ Nm}$

vector1 = 40%

vector2 = 80%

vector3 = 100%

Fig. 9 – Estimated torque response for modified torque hysteresis.

Fig. 9 shows torque response for three different hysteresis bands: 0.1 Nm, 0.3 Nm and 0. Nm, respectively, with three voltage vectors according to Fig. 8. It can be noticed that the torque ripple decreases as hysteresis band increases.

Influence of this hysteresis modification on torque ripple was analyzed using three voltage vector intensities: 40%, 80% and 100%. Estimated torque is shown in Fig. 9 for three different hysteresis bands and the same torque reference of 0.4 Nm.

When the hysteresis band is wider the estimated torque often takes values in the hysteresis range with different intensities of corresponding voltage vector. In this way it is possible to reduce torque ripple. Nevertheless, quick torque response is maintained for large values of torque error when full voltage vector is applied.

The disadvantage of the conventional hysteresis comparator is that the electromagnetic torque decreases when zero voltage vector is applied. In such cases, angle between stator and rotor vector flux decreases and consequently electromagnetic torque decreases too. Fig. 5 shows decreasing of torque during zero voltage vector which proves previous assumption. This is especially evident in case of low power motors with low value of rotor time constant. Therefore, zero voltage vector can be referred to as the vector that decreases torque. Consequently the average value of electromagnetic torque is lower than the torque reference. Modified hysteresis comparator can reduce consequences of this drawback if vector intensities are appropriately rearranged in hysteresis comparator as shown in Fig. 10.

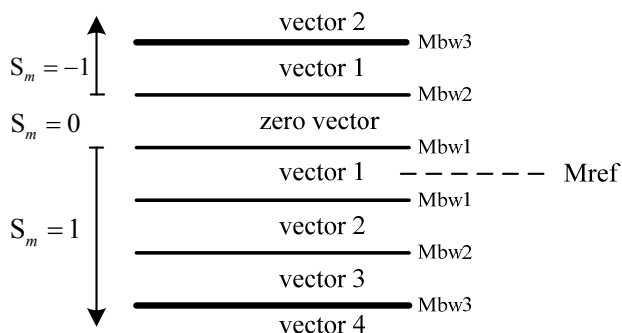


Fig. 10 – Reallocation of voltage vectors in modified hysteresis comparator.

The torque responses with modified comparator (Fig. 10) during the same conditions are shown in Fig. 11.

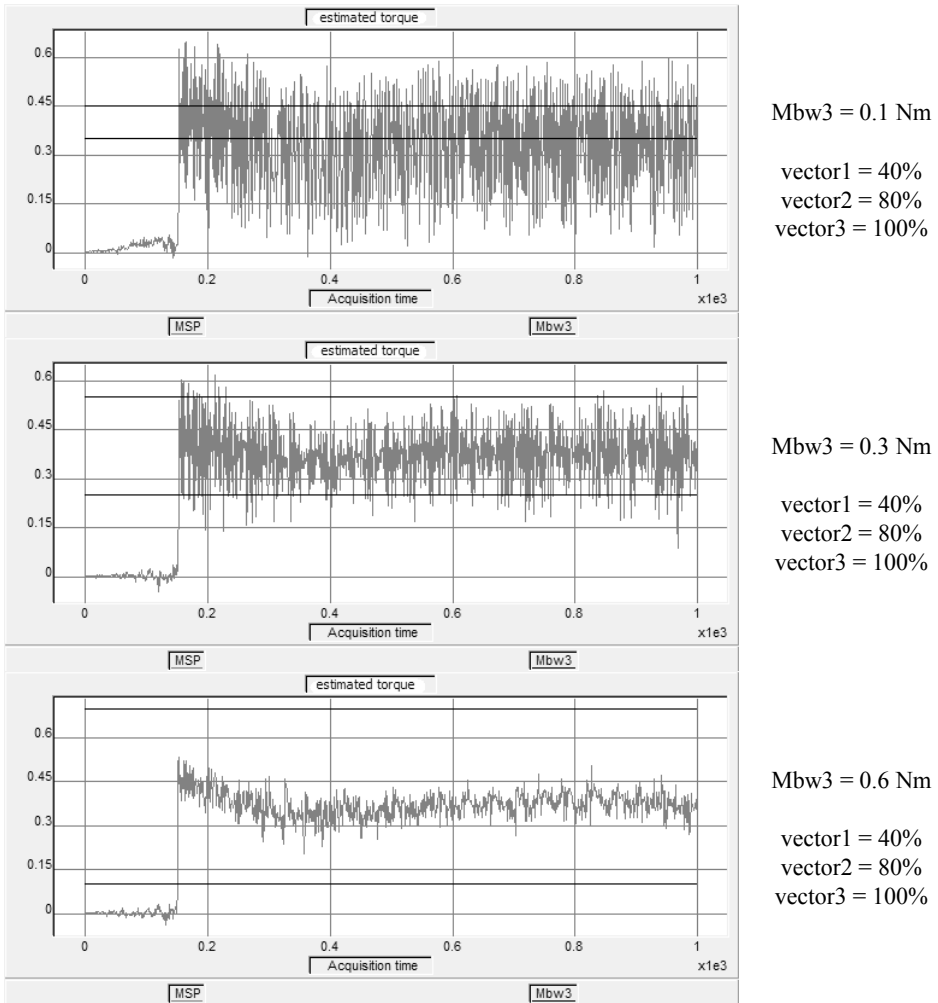


Fig. 11 – Estimated torque response for modified hysteresis comparator and relocated voltage vectors.

Fig. 11 confirms advantages of this method with modified hysteresis comparator and adjustable voltage vectors. The torque ripple is significantly reduced and its average value corresponds to the reference value of 0.4 Nm. Also, lower level of acoustic noise is noticed as a consequence of torque and current ripple reduction (Fig. 12).

Fig. 12 shows stator currents in stationary α and β axis in cases with classic DTC (with full voltage vector) and with proposed DTC algorithm (variable voltage vectors and modified hysteresis). It can be seen that current ripple is significantly reduced.

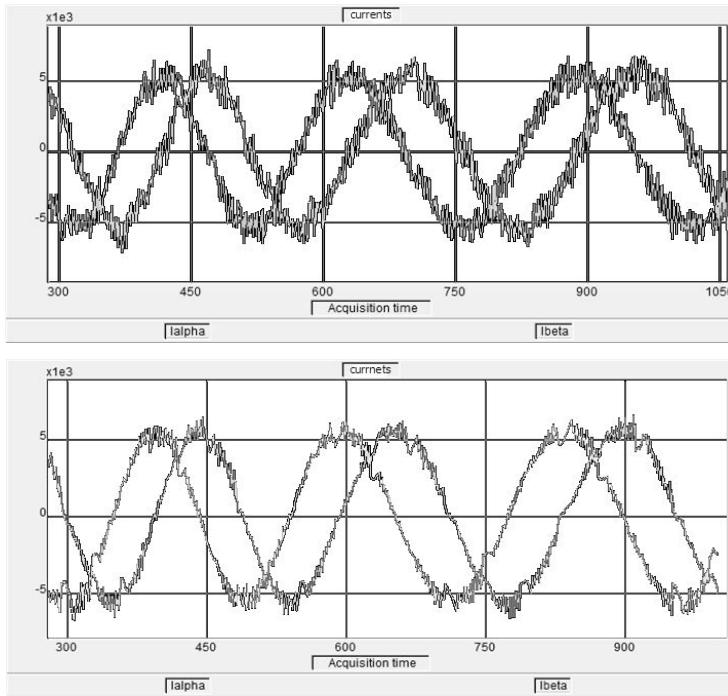


Fig. 12 – Stator currents with classic DTC (top) and with proposed DTC method (bottom).

With only three different voltage vector intensities torque and current ripple are reduced by three times, compared to the results with full voltage vector. In this way, by analogy, it is possible to define higher number of voltage vectors and hysteresis comparator with higher number of segments. This will further contribute to the torque ripple reduction.

5 Conclusion

This paper analyses the effect of variable intensity discrete voltage vectors to the torque ripple reduction in direct torque control of low power induction motors. Analyses are performed through the implementation on MSK2812 DSP based system. Experimental results are presented and discussed. The advantages of the proposed algorithm are verified in the reduced ripple of the estimated torque. Torque and current ripple are significantly reduced and simplicity of the basic DTC algorithm is maintained, without the need for rotating transformations and PI regulators. Also, unlike the classical DTC method, the introduction of the pulse width modulation defines constant switching frequency. Further research will investigate the correspondence between voltage

vector intensity and the flux and torque errors to achieve maximum torque ripple reduction with minimum number of segments in the comparator.

6 Acknowledgement

This paper is a result of activities within the project TR33016 which is supported by Ministry of Education and Science and Technological Development of Republic Serbia.

7 References

- [1] I. Takahashi, T. Noguchi: A New Quick-response and High-efficiency Control Strategy of Induction Motor, IEEE Transaction on Industry Applications, Vol. IA-22, No. 5, Sept. 1986, pp. 820 – 827.
- [2] P. Matić, B. Blanuša, S.N. Vukosavić: Direct Torque Control and Field Oriented Control in μ C Drives, INFOTEH, Jahorina, Republic of Srpska, BIH, 25 – 27 March 2002, Vol. 2, Ref. D-2, pp. 227 – 231.
- [3] P. Vas: Sensorless Vector and Direct Torque Control, Oxford University Press, NY, USA, 1998.
- [4] V.N. Katsikis: MATLAB - A Fundamental Tool for Scientific Computing and Engineering Applications - Volume 1, InTech, Rijeka, Croatia, 2012.
- [5] S. Belkacem, F. Naceri, R. Abdessemed: Reduction of Torque Ripple in DTC for Induction Motor using Input-output Feedback Linearization, Serbian Journal of Electrical Engineering, Vol. 8, No. 2, May 2011, pp. 97 – 110.
- [6] P.L. Jansen, R.D. Lorenz: A Physically Insightful Approach to the Design and Accuracy Assessment of Flux Observers for Field Oriented Induction Machine Drives, IEEE Transaction on Industry Applications, Vol. 30, No. 1, Jan/Feb. 1994, pp. 101 – 110.
- [7] N.T. West, R.D. Lorenz: Digital Implementation of Both a Stator and Rotor Flux Linkage Observer and Stator Current Observer, 42nd IEEE Industry Applications Society Annual Meeting, New Orleans, LA, USA, 23 – 27 Sept. 2007, pp. 1001 – 1007.
- [8] Technosoft MCK2812 Technical Data and User Manual. Available Online: <http://www.technosoftmotion.com/en/tools/professional-kits-with-apps/induction-motor-control-kits/mck2812-kit-c-pro-s-im>
- [9] H.I. Okumus, M. Aktas: Adaptive Hysteresis Band Control of Constant Switching Frequency in DTC Induction Motor Drives, Turkish Journal of Electrical Engineering and Computer Sciences, Vol. 18, No. 1, Jan. 2010, pp. 59 – 69.
- [10] J.K. Kang, D.W. Chung, S.K. Sul: Direct Torque Control of Induction Machine with Variable Amplitude Control of Flux and Torque Hysteresis Band, Electric Machines and Drives, International Conference Electric Machines and Drives, Seattle, WA, USA, 09 – 12 May 1999, pp. 640 – 642.
- [11] F. Khoucha, K. Marouani, A. Kheloui, K. Aliouane: A DSP-based Discrete Space Vector Modulation Direct Torque Control of Sensorless Induction Machines, Nordic Workshop on Power and Industrial Electronics, Trondheim, Norway, 14 – 16 June 2004, p. 025.